Roll-Performance Criteria for Highly Augmented Aircraft

Mario Innocenti* and Ajay Thukral†
Auburn University, Auburn, Alabama 36849

Highly augmented fly-by-wire aircraft have shown a degradation in roll performance during compensatory tasks such as tracking, similar to the ones observed for the pitch axis. Gibson's method, which involves a combination of time-domain and frequency-domain techniques, has been shown to provide excellent handling-qualities criteria for the pitch axis, especially in identifying pilot-induced oscillations. The present work extends Gibson's method to develop similar handling-qualities criteria for the roll-axis control system. The effects of parameters such as roll damping, transport delay, system gain, and corresponding pilot ratings are studied for developing handling-qualities criteria and to evaluate the flight-control system performance. Flying-qualities levels are obtained in both the time and the frequency domain. In addition, frequency-domain analysis is used to identify pilot-induced oscillation-prone configurations and the presence of roll ratcheting. The analysis is performed and validated using an existing experimental data base on lateral flying qualities of highly augmented class IV aircraft.

Nomenclature

e	= natural exponential
K	= pilot gain
$L'_{F_{as}}$	= roll-control effectiveness
P_r	= phase rate
P_{ss}	= steady-state roll rate
$q_{\max}$	= maximum pitch rate
q_{ss}	= steady-state pitch rate
R_a	= acceleration ratio
s	= complex number
Y_p	= pilot transfer function
δ_a	= aileron deflection
ζ_{sp}	= short period damping
θ_{db}	= pitch attitude dropback
θ_{ss}	= steady-state pitch angle
θ_5	= pitch angle at time $t = 5$ s
τ	= time constant
τ_d	= pure time delay
τ_{eff}	= effective time delay
τ_r	= roll time constant
$\dot{\phi}_{\max}$	= maximum roll acceleration
ϕ_{nos}	= normalized bank-angle overshoot
ϕ_5	= roll angle at $t = 5$ s
ω	= frequency
ω_{sp}	= short period frequency
$\omega_{0.3}$	= frequency at 0.3 Hz
ω_{180}	= frequency at phase lag = 180 deg
ω_{200}	= frequency at phase lag = 200 deg

I. Introduction

THE importance of stability augmentation to the success of modern high-performance aircraft is fundamental. Flight tests and simulations with aircraft having high-order dynamics due to control systems, digital implementation, etc., have been very promising in terms of command response, precision controllability, and hands-off operation. Handling-qualities deficiencies, however, have surfaced due to generic problems such as oversensitivity to small control inputs and sluggish response to large inputs. Improper control gains and time delays coupled with higher-order effects have resulted in low-frequency pilot-induced oscillations (PIO) and high-frequency ratcheting interaction.[1]

As reflected in the latest military specifications,[2,3] the majority of the work in handling-qualities research has been limited to longitudinal motion. Among the reasons were the recognition of the longitudinal plane as the primary plane in closed-loop control tasks, the availability of a large experimental data base, and the introduction of aircraft with a high level of longitudinal augmentation due to relaxed static stability.

A comprehensive technique for longitudinal handling-qualities analysis and assessment has been developed over the years by Gibson at British Aerospace Corporation[4-6] using experience acquired in the experimental aircraft program (EAP) and in the development of aircraft such as the Jaguar fly-by-wire (FBW) and the Tornado. The main objectives of Gibson's derivations (also referred to as the dropback method) are the explanation and prediction of PIO experienced during critical flight phases of highly augmented aircraft. Good correlation has been obtained with the dropback method in matching pilot opinions to aircraft characteristics in tracking and landing for military[4,5] as well as transport aircraft.[7] Agreement with the new longitudinal handling-qualities specifications has also been reported.[8,9]

Traditionally, lateral dynamic characteristics have not been considered critical in the assessment of the overall handling qualities. Specifications for the roll response, for example, are based essentially on open-loop-type parameters such as roll time constant, maximum roll rate, and time to go through a bank angle for roll control effectiveness.[2,3] Lateral handling qualities, however, are becoming more important in relation to increased control-system augmentation level at high angle of attack, to pitch-roll coupling during loaded maneuvers, and to agility requirements. In addition, recent experimental results[10] showed the presence of low-frequency pilot-induced oscillations in roll (due to mismatch between roll zeros and poorly damped dutch roll) and high-frequency ratcheting.[11] To the author's knowledge, no guidelines are presently available that can help the designer in predicting the occurrence of the above instabilities.

The objectives of the present work are to extend Gibson's method to the roll axis so as to identify metrics and handling-qualities boundaries for satisfactory dynamic behavior of the flight control system (FCS). The paper is organized as follows: Sec. II will briefly review the main ideas behind Gibson's method; Sec. III will discuss roll axis requirements and briefly talk about lateral high-order systems (LATHOS) and its ex-

Received Nov. 30, 1989; revision received Aug. 1, 1990; accepted for publication Oct. 2, 1990.

*Associate Professor, Department of Aerospace Engineering. Senior Member AIAA.

†Graduate Student, Department of Aerospace Engineering. Student Member AIAA.

perimental setup; and the last two sections will present the analysis and conclusions.

II. Review of Gibson's Method

Gibson's method has grown over the years to encompass most of the classical approaches to the handling-qualities problem.[4-6] In his earlier work, Gibson addressed some of the deficiencies of the specifications in dealing with higher-order aircraft, deficiencies that surfaced during the development of the digital FCS for the Jaguar FBW and the Tornado aircraft. The major concern was the difficulty in identifying lower-order modal parameters such as short-period damping and natural frequency, control anticipation parameter (CAP), and flight-path delay constant to which the military specifications (MIL-SPEC) are applicable. The problem has been a common one among flying-qualities researchers, leading to other accepted approaches such as the bandwidth criterion[12] and equivalent systems.[13]

The basic idea behind Gibson's method is that of achieving good classical airplane characteristics in the presence of high-order effects due to augmentation. The FCS should be designed to have not only classical response but also to satisfy the specific task requirements. It is clear that easily and directly identifiable metrics are required instead of specifications given in terms of modes. These would then encompass both classical and modern airplanes in a more straightforward manner. Gibson's method combines time-response and frequency-response techniques to cover the frequency spectrum of interest to the pilot. Thus, time response to a block step input describes low-to-medium frequency range and is representative of low-range frequency tasks such as pursuit tracking and flight-path tracking. On the other hand, frequency response at very low frequencies is unreliable due to insufficient input power. The frequency response best justifies its use around the crossover region for tight tracking and for higher frequencies, and it is similar in the approach to the evaluation of the equivalent time delay.[13]

Gibson's time-domain analysis looks at attitude, pitch rate, and acceleration responses to a block-type stick input. The behavior of the initial response at the time of stick release is related to pilot comments. Gibson's frequency-domain analysis, based on Nichols' charts of the open-loop response with pure gain manual compensation, highlights PIO tendencies by relating such instability to the phase rate at -180 deg and its corresponding phase-lag crossover frequency. Parameters such as dropback, overshoot, and phase rate can be easily obtained. These are related to typical short-period dynamics comments like bobbling, sluggishness, and induced instability. Gibson's criterion is briefly summarized in the next paragraphs and the interested reader can also refer to Refs. 4-6, 8, and 14 for more details.

A pitch-angle time history to a block input is required to determine the attitude dropback as shown in Fig. 1 (taken from Ref. 5). The dropback θ_{db} is defined by

$$\theta_{db} = \theta_5 - \theta_{ss} \tag{1}$$

where θ_{ss} is the steady-state pitch angle and θ_5 is the value of pitch angle when the block input is zeroed. The main requirement is that the attitude dropback normally be positive (no overshoot). Normal acceleration-response boundaries can also be used that are in fact a direct translation of traditional short-period requirements (Sec. 3.2.2 from Ref. 2).[5-6] The qualitative nature of the analysis is evident in that the time-domain results are mainly used to correlate with pilot comments relative to a response type (such as sluggishness, quickness, bobbling, ability to maintain target, etc.) and not to obtain handling-qualities levels.

The attitude-frequency response is used to highlight potential PIO prone configurations. This idea closely follows earlier pilot-in-the-loop compensatory tracking studies done by McRuer and co-workers at STI and by Neal and Smith at Calspan. Frequency response in tracking considers the pilot behavior represented by a pure gain and time delay, with transfer function $Y_p = Ke^{-\tau s}$, where τ is the pilot's time delay constant, usually of the order of 0.2 s (these are typical experimental values for the pilot in compensatory tracking tasks). The gain K for the tracking task is adjusted so as to obtain a gain crossover frequency of 0.3 Hz. In the case of an approach and landing task, the gain K is adjusted so as to have a phase lag of 120 deg at the gain crossover point.

Considerable success has been obtained in identifying PIO using attitude-frequency boundaries. Analysis of tracking as well as landing tasks reveals that the main parameter leading to PIO identification is the phase rate P_r, defined as

$$P_r = 20/(\omega_{200} - \omega_{180}) \quad \text{deg/Hz} \tag{2}$$

where the frequency is measured in Hertz. High phase-rate values are invariably related to large time delays, thus indicating the presence of a PIO prone configuration.

As an example, handling-qualities analysis is performed for a transport aircraft (E-1 configuration from Ref. 7) and a class IV aircraft (1-3 configuration from Ref. 15) during approach

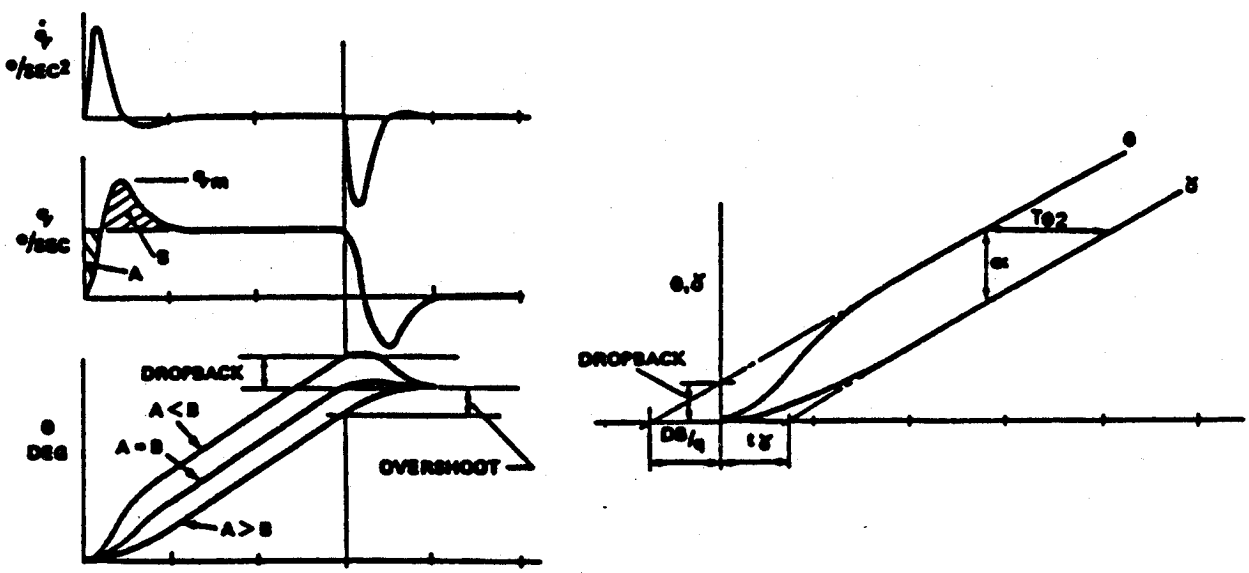

Fig. 1 Longitudinal dropback time responses (from Ref. 5).

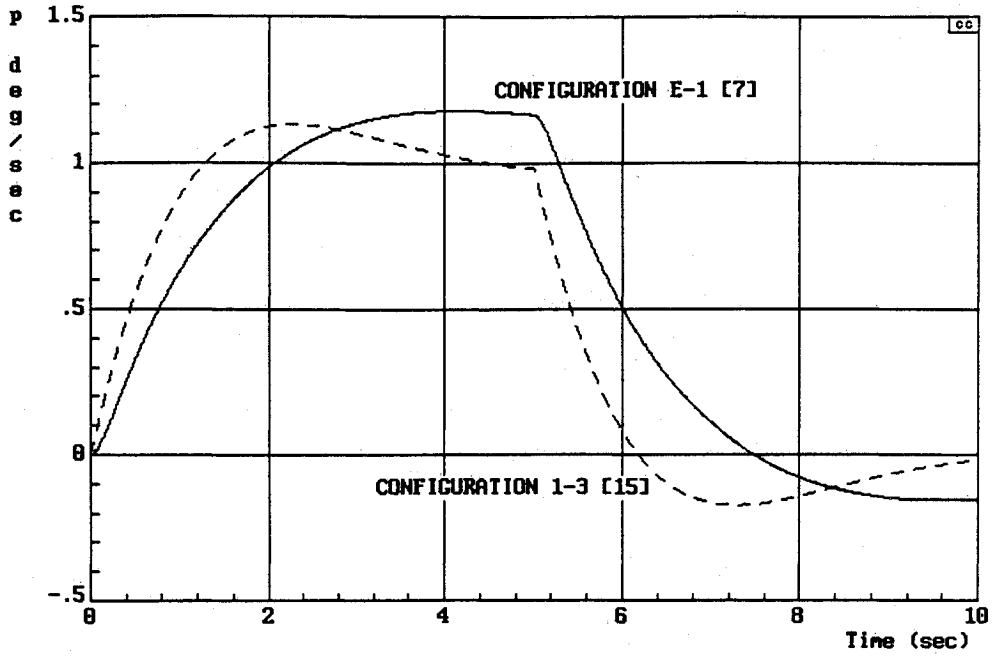

Fig. 2 Pitch rate response to block input.

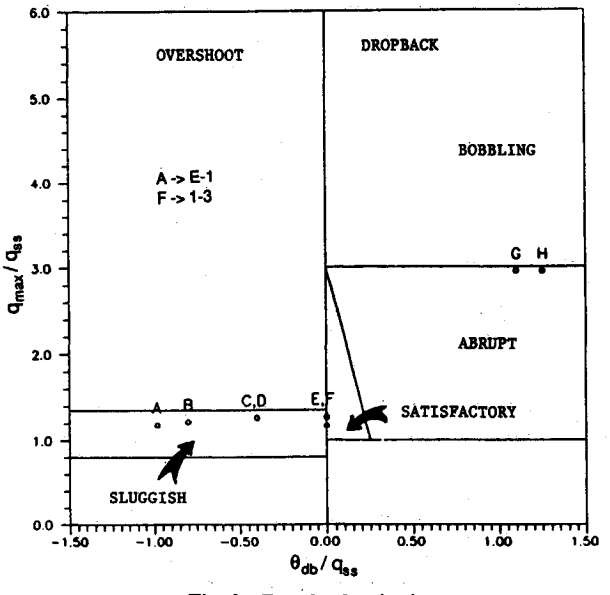

Fig. 3 Dropback criteria.

and landing tasks. These aircraft have ratings of level 3 and level 1, respectively. The primary parameter for the study was the short-period natural frequency that affects the rise time and bandwidth of the configurations. A typical time history used for time-response evaluation is shown in Fig. 2 corresponding to configurations E-1 and 1-3. The time response is summarized by the dropback criterion shown in Fig. 3 where the configurations are plotted (marks A and F) in terms of normalized maximum pitch rate vs θ_{db}/θ_{ss}. A qualitative handling-quality behavior can be obtained from the figure, where the regions roughly represent areas of similar comments made by the pilots. As shown, configuration E-1 ($\zeta_{sp} = 0.74$, $\omega_{sp} = 0.5$) is a level 3, whereas configuration 1-3 ($\zeta_{sp} = 0.74$, $\omega_{sp} = 1.0$) is a level 1 consistent with the experimental results.[7-15]

Nichols charts for configurations E-1 and 1-3 are given in Fig. 4. The boundaries identifying satisfactory behavior are determined according to Ref. 4 for the approach and landing task. Configuration 1-3 shows a well-behaved frequency response, whereas configuration E-1 suggests a sluggish response and a high phase rate ($P_r = 289$ deg/Hz), which indicates PIO. Consistent comments were recorded during the experiments in Refs. 7 and 15.

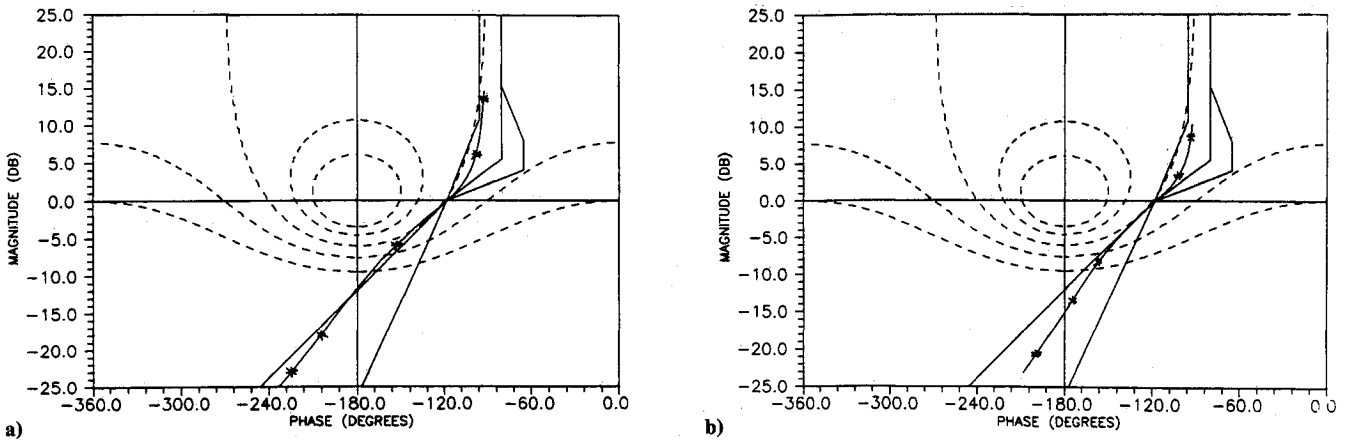

Fig. 4 Frequency response boundaries for pitch axis: a) configuration E-1 and b) configuration 1-3.

Table 1 Pilot ratings and comments from LATOS

Case	Mean pilot rating-level	Symbol	τ_r, s	τ_d, s	p_{ss} F_{as}	Pilot comments[a,b,c]
(TR)1-3	3/L1	A	0.8	0.00	18	NPio,NRa,GIR,GFR,GAg,GP,GFt,GSen
(TR)1-3T1	7/L3	B	0.8	0.03	18	Pio,NRa,SIR,GAg,BP,BFt,LSenL
(TR)1-3T2	8/L3	C	0.8	0.06	18	Pio,NRa,SIR,GFR,BAg,BP,BFt,LSen
(TR)1-2	5/L2	D	0.8	0.00	10	NPio,NRa,SIR,BFR,GAg,BPL,GFt,SSen
(TR)2-3	3/L1	E	0.45	0.00	18	NPio,NRa,GIR,GFR,GAg,GP,GFt,GSen,HSenS
(TR)2-3T1	4.5/L2	F	0.45	0.03	18	Osc,NPio,NRa,QIR,OFR,BAg,OP,GFt,HSen
(TR)2-3T2	5.5/L2	G	0.45	0.06	18	Osc,NPio,NRa,QIR,BAg,BP,BFt,HSen
(TR)2-3T3	8.5/L3	H	0.45	0.08	18	Osc,Pio,SIR,QFR,BAg,BP,BFt,LISen,HFSen
(TR)2-2	3/L1	I	0.45	0.00	10	NPio,NRa,SIR,OFR,GAg,GP,GFt,OSen
(TR)2-2T1	2/L1	J	0.45	0.03	10	NPio,NRa,GIR,GFR,GAg,GP,GFt,GSen
(TR)2-2T2	5.5/L2	K	0.45	0.06	10	NPio,NRa,SIR,OFR,BAg,BP,BFt,LSen
(TR)2-2T3	7/L3	L	0.45	0.08	10	Pio,NRa,NIRS,OIRL,GFRL,BAg,BPS,GPL,OSen
(TR)2-2T4	8/L3	M	0.45	0.18	10	Osc,Pio,NRa,BIR,BFR,BAg,BP,BFt,LSen
(TR)3-3	5/L2	N	0.25	0.00	18	Osc,Pio,Ra,QIR,OFR,BAg,OP,BFt,HSenS
(TR)3-3T2	7/L3	O	0.25	0.06	18	Ra,QIR,BFR,BAg,BP,HSen
(TR)3-3T3	7/L3	P	0.25	0.08	18	Ra,QIR,BFR,BAg,OP,GFt,HSen
(TR)3-2	3.5/L1	Q	0.25	0.00	10	NPio,NRa,GIR,GFR,GAg,GP,OFt,NSen(about neutral)
(TR)5-3	7/L3	R	0.15	0.00	18	Osc,Ra,QIR,GFR,BAg,BP,BFt,LISen,HFSen
(TR)5-3T1	7/L3	S	0.15	0.03	18	Osc,Ra,QIR,OFR,BAg,BP,BFt,HSen
(TR)5-3T2	8/L3	T	0.15	0.06	18	Osc,Pio,QIR,BFR,BAg,BP,HSen
(TR)5-2	7/L3	U	0.15	0.00	10	Osc,Ra,QIR,BFR,BAg,BP,BFt,OSen
(TR)5-2T1	7/L3	V	0.15	0.03	10	Osc,Ra,BAg,HSenS
(TR)5-2T3	8/L3	W	0.15	0.08	10	Osc,Ra,QIR,OFR,BAg,BP,HSen
(TR)2-4	3.5/L1	A1	0.45	0.00	25	NPio,NRa,GIR,GFR,GAg,GP,GFt,LISen,OFSen
(TR)2-4T1	5/L2	A2	0.45	0.03	25	OSc,Ra,QIR,OFR,BAg,BP,BFt,HSenS
(TR)2-4T2	6/L2	A3	0.45	0.06	25	Pio,Ra,QIR,OFR,BAg,BP,HSen
(TR)2-4T3	9/L3	A4	0.45	0.08	25	Pio,BIR,BFR,BAg,BP,HSen
(TR)3-4	6/L2	A5	0.25	0.00	25	Osc,NPio,NRa,QIR,OFR,BAg,BP,BFt,HSen
(TR)3-4T2	7/L3	A6	0.25	0.06	25	Osc,NPio,Ra,QIR,BAg,BP,HSen

[a]Prefix: N = no; G = good; B = bad; S = sluggish; Q = quick/jerky; L = low; and H = high.
[b]Root: Pio = pilot-induced oscillation; Ra = ratcheting; R = response; Ag = agressiveness; P = predictability; Ft = fine tracking; Sen = sensitivity; Osc = oscillation; IR = initial response; and FR = final response.
[c]Suffix: L = large input; and S = small input.

III. Roll-Response Requirements and Data Base

The limitations of lateral handling qualities with respect to high-performance aircraft have been acutely felt since the MIL-SPEC-8785C, which, while being used for both design and testing of developing aicraft, failed to provide the desired handling qualities. These limitations could be attributed to a limited data base that mainly represented aircraft of the World War II era, which had limited or no lateral augmentation. The need for identifying problems related to a lateral highly augmented fighter aircraft led to a series of in-flight simulations to generate experimental data and to investigate the effects of lateral high-order systems (LATHOS).[10] The additional insight gained through the LATHOS experiment provided a large enough data base for the revision of MIL-SPEC-8785C. Currently, MIL-STD-1797 presents the desired requirements in a format similar to the older specification and, at the same time, provides the necessary guidance for highly augmented systems.[3]

The present paper suggests new roll-response metrics based on the application of Gibson's method to the LATHOS data base and presents qualitative as well as quantitative relationships between pilot ratings and typical parameters such as roll time constant, time delay, and control system gain, which constitute the scope of the present analysis. In addition to these parameters, the LATHOS experiment examines several others, such as lead-lag time constants, nonlinear command

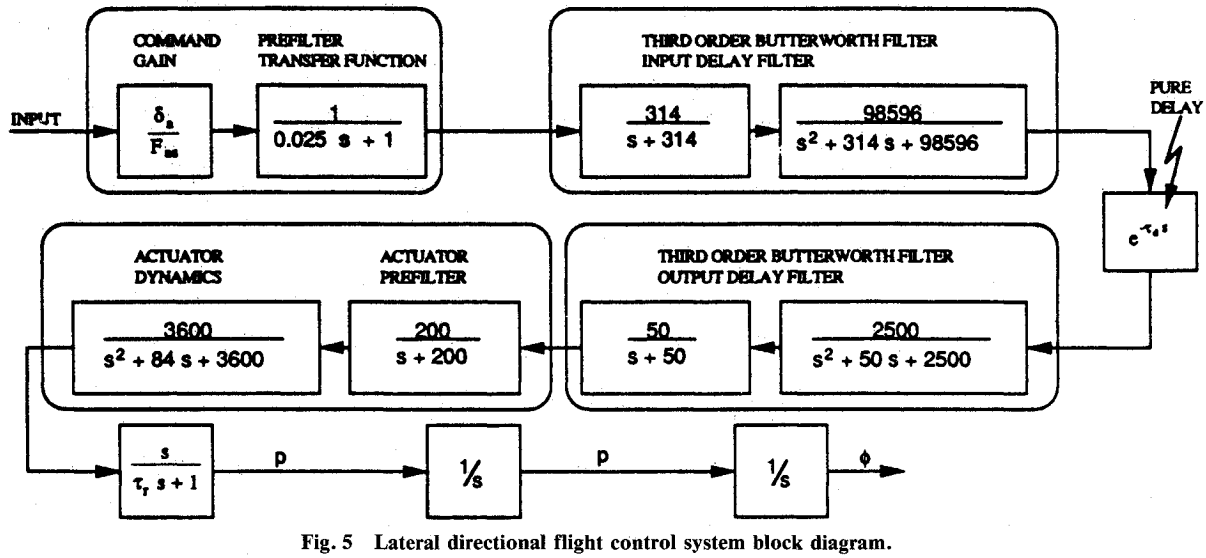

Fig. 5 Lateral directional flight control system block diagram.

shaping characteristics, and dutch-roll damping, that will not be considered herein. Figure 5 shows the modified block diagram of the lateral-direction flight control system for the stick-roll loop only. The three primary variables are shown by their corresponding symbols, linear command gain δ_a/F_{as}, roll time constant τ_r, and pure time delay τ_d. The time delay τ_d is the pure time delay generated by the NT-33A's time delay circuit that merely holds the signal by τ_d seconds. This could be thought of as representing delays due to various possible sources such as structural lag, transport lag, and digital delays present in actual system. The filters surrounding the time-delay circuitry are third-order Butterworth low-pass filters that help in smoothing the signal. The dutch-roll characteristics and the lead-lag time constants were held to their nominal value. Typical first-order response for the aircraft is assumed to be given by the transfer function

$$\frac{p}{F_{as}} = \frac{\tau_r L'_{Fas}}{(\tau_r s + 1)} \tag{3}$$

in which the dutch-roll mode is absent due to the dipole effect and the spiral mode is absent due to a large time constant. The roll requirements and justifications for the primary parameters are as follows:

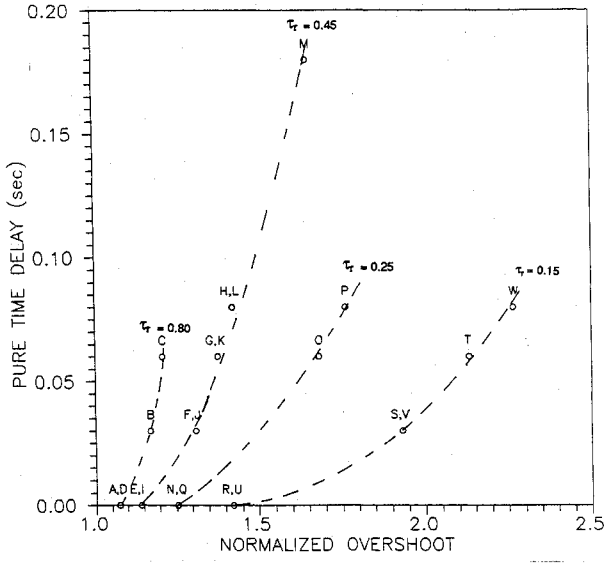

Fig. 6 Time-response analysis results with no sensitivity.

1) The roll-damping requirement given by MIL-STD-1797 limits the lower damping to 0.3 s ($0.3 \le \tau_r \le 1$ s for level 1). These results are supported by the fact that some modern aircraft equipped with high gain augmentation have time constants that are too small and experience an excessive lateral sensitivity described as roll ratcheting.

2) The time delay in a control system can drastically degrade lateral flying qualities. The MIL-STD-1797 retains the pure time delay limits given in the 8785C, mainly because of a lack of supporting data to revise them, which limits maximum delay to 0.1 s for level 1 and no more than 0.2 s for level 2.

3) A very important parameter that has not been dealt with in sufficient depth is the effect of command gain δ_a/F_{as}. Earlier metrics normally excluded the effect of this open-loop gain variation, as it was considered an independent variable to be optimized. Usually the gain is very critical to the pilot in that it changes his/her equalization, and it is known to contribute greatly to the pilot opinion and ratings. Hence, the roll metrics developed in this paper include the effect of command-gain variation along with other roll parameters. Roll-control sensitivity and roll-control effectiveness are directly related to command gain δ_a/F_{as}. We define roll-control sensitivity as the gain required by the steady-state roll rate p_{ss} to a unit step input. Roll-control effectiveness L'_{Fas} is defined as roll-control sensitivity per unit roll time constant, or

$$L'_{Fas} \doteq p_{ss}/\tau_r \tag{4}$$

Tasks performed during the LATHOS experiment were representative of flight phase categories A and C and consisted of actual target tracking, air refueling, precision approach and landing, as well as special head up display (HUD) tracking tasks. The results of the experiment are documented in Ref. 10 with time histories, pilot comments, and data correlation.

The complete set of configurations for the tracking task, constituting all of the configurations with linear gain only, were analyzed (29 cases in all) as well as most of the landing configurations. Throughout the analysis the pilot is assumed to be described by a pure gain element. Table 1 lists all of these configurations along with the values for the variables, pilot comments, and the pilot ratings based on the Cooper-Harper scale. Only tracking task results will be presented in the paper.

IV. Time-Response Analysis

Several new metrics are needed to characterize the roll handling qualities. Gibson's metrics such as dropback θ_{db}, the effective time delay θ_{db}/q_{ss}, and $q_{\max}/q_{ss}$ are no longer directly

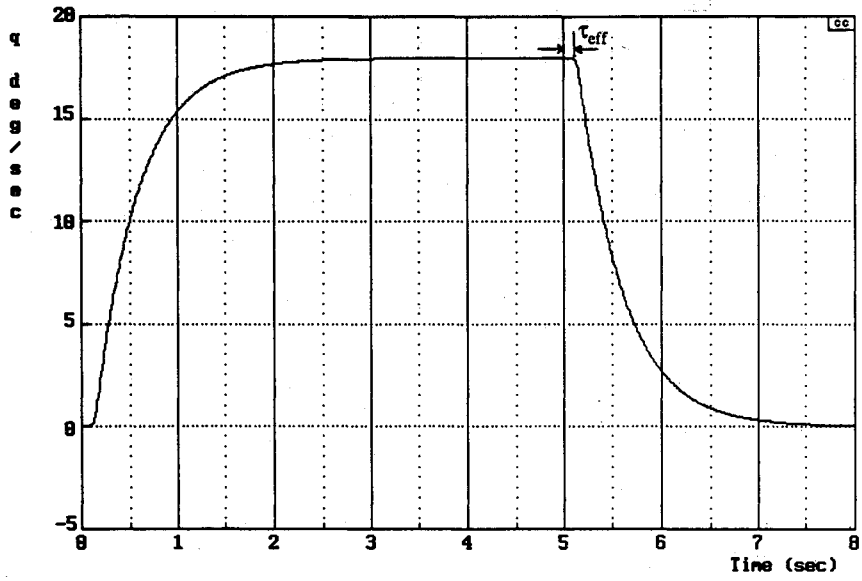

Fig. 7 Effective time delay τ_{eff}.

applicable due to the basic difference between pitch and roll responses and the inclusion of control system command gain.

The metrics that were considered are the effective time delay τ_{eff}, the roll-control effectiveness p_{ss}/τ_r, and the acceleration ratio R_a. Parameters such as maximum acceleration $\ddot{\phi}_{\max}$ are also used in the analysis. The parameters related to roll axis are mainly acceleration dependent since experiments have shown that the pilot responds to acceleration cues sensed by his/her vestibular sensory system. These experiments have also shown pilots' aversion to high roll acceleration.

The basic roll response to step input is of a first-order type and hence consists of overshoot only (in the context of Fig. 1). The traditional definition of dropback is now replaced by normalized bank-angle overshoot ϕ_{nos}, and is given by

$$\phi_{nos} = \frac{\phi_{ss} - \phi_5}{\phi_{ss}\tau_r} \tag{5}$$

where ϕ_{ss} is the steady-state bank angle, and ϕ_5 is the bank angle at time $t = 5$ s (time of block input release). However, it is seen that direct use of Eq. (5) for the normalized overshoot, although similar in nature to dropback, is not helpful since ϕ_{nos} is independent of roll-control sensitivity, and by its direct relation to pilot comments no correlation is observed. The determination of a metric involving roll-control sensitivity is not straightforward. This is so because the use of any normalized metric data comparison leads to the elimination of loop gains and hence can lead to misleading results. As an example, Fig. 6 shows the behavior of ϕ_{nos} vs time delay τ_d for similar configurations. With different roll-control sensitivity only (18 and 10, respectively), similar handling-qualities characteristics would be deduced for the overlapping configurations (A, D; E, I; F, J; G, K; H, L; N, Q; R, U; S, V), although pilot ratings and comments are markedly different for these cases, thus showing how control sensitivity effects pilot opinion.

The pure time delay τ_d does not account for the effect of higher-order dynamics. To overcome this difficulty, an effective time delay τ_{eff} is defined as the time taken by the system to respond to a change in forcing function, and it is the sum of pure time delay τ_d and delays due to the presence of other higher-order terms. The parameter τ_{eff} represents the actual response delay as seen by a pilot, and it is shown in Fig. 7. This parameter is similar to τ_{eff} defined in Ref. 10. The difference lies only in the way it is measured.

Roll-control effectiveness p_{ss}/τ_r, also represented by L'_{Fas} in Eq. (3), is used to compute initial roll acceleration. This could be derived by applying the initial-value theorem to the roll-acceleration transfer function; hence the terms roll-control effectiveness and initial acceleration are used interchangeably depending on the context.

As will be shown, a good correlation exists between τ_{eff}, p_{ss}/τ_r, and pilot ratings, which is similar to the longitudinal

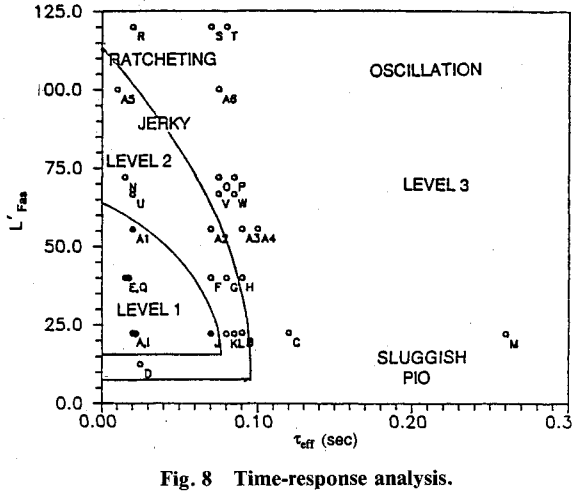

Fig. 8 Time-response analysis.

Table 2 Summary of metrics

Metric	Description	Usage
τ_{eff}	Effective time delay	Boundaries of Fig. 8
$L_{F'as}$	Initial roll acceleration p_{ss}/τ_r	Boundaries of Fig. 8
R_a	Roll-acceleration ratio	$0.91 > R_a > 0.71$ (for normal roll response)

case (θ_{db}/q_{ss}, $q_{\max}/q_{ss}$) as pointed out in previous work by Rynaski.[16] Some anomalies exist, but these were found to be related to the acceleration ratio R_a, defined as the ratio of maximum acceleration $\ddot{\phi}_{\max}$ (measured from the block step-response simulation of the entire system) to initial acceleration p_{ss}/τ_r (computed from the roll-acceleration transfer function), and given by

$$R_a = \frac{\ddot{\phi}_{\max}}{p_{ss}/\tau_r} \tag{6}$$

The configurations listed in Table 1 were simulated in terms of bank angle, roll rate, and roll-acceleration time responses. Based on the metrics discussed above, the results of the analysis are shown in Fig. 8.

Figure 8 relates effective time delay τ_{eff} to initial acceleration p_{ss}/τ_r. Clearly, initial acceleration is a function of roll-control sensitivity p_{ss} and the roll time constant τ_r. On the other hand, τ_{eff} is mainly a function of pure time delay τ_d. Qualitative boundaries are drawn in Fig. 8 showing lower and upper bounds on p_{ss}/τ_r. From a physical standpoint, a sufficient threshold value is required for the initial acceleration in order for the response to be sensed by the pilot. However, too large a value is not acceptable. Comments such as quick and jerky responses are typified. For any given level of flying qualities, the threshold value for the initial acceleration remains constant (for level 1 L'_{Fas} is >15), although the upper limit is seen to decrease with increase in effective time delay τ_{eff}.

Let us consider a few typical cases and analyze the initial acceleration parameter p_{ss}/τ_r from a different viewpoint. Configurations A, E, N, and R all have constant roll-control sensitivities but decreasing roll time constants τ_r. Thus, the roll-control sensitivity p_{ss}/τ_r increases as τ_r (inversely proportional to τ_r) decreases with constant control sensitivity. The new MIL-STD-1797 conditions specify a lower limit for τ_r. For $\tau_r < 0.3$ s, ratcheting is predicted. Thus, cases A and E do not have ratcheting as $\tau_r > 0.3$ s, whereas cases N and R do ($\tau_r < 0.3$ s).

Now consider cases F, J, and A2 that have $\tau_r = 0.45$ s ($\tau_r > 0.3$ s), but vary roll-control sensitivity. In this case, A2 exhibits ratcheting deficiency due to high roll-control sensitivity. In conclusion, configurations with $\tau_r < 0.3$ s will always have ratcheting, but for $\tau_r > 0.3$ s, ratcheting may or may not occur depending on roll-control sensitivity. The frequency analysis also corroborates the statement. From Fig. 8, for zero time delay, we obtain the following limits on L'_{Fas}:

$$15 < L'_{Fas} < 60 \qquad \text{for level 1} \tag{7a}$$

$$7.5 < L'_{Fas} < 110 \qquad \text{for level 2} \tag{7b}$$

The effective time delay τ_{eff} affects roll handling qualities in a fashion similar to θ_{db}/q_{ss} for the pitch axis. Large time delays slow down the response and force an oscillatory response from the pilot. Configurations C and M have large time delays. Both are commented as slow-responding aircraft and exhibit definite PIO in precision maneuvers. For level 1 criteria, the effective time delay τ_{eff} is limited to less than 0.07 s. In the case of configurations with higher roll-control sensitivity (coupled by large time delays), pilot comments about oscillatory motion, shown in Fig. 6, border between the PIO and ratcheting regions.

Some anomalies do exist and, as mentioned earlier, agreement with the boundaries is observed if a given configuration satisfies the inequality

$$0.91 > R_a > 0.71 \tag{8}$$

Failure to satisfy Eq. (8) yields relatively poor pilot ratings compared to neighboring points. Configurations B and U are typical in this respect. They both have level 3 handling qualities but lie very close to configurations N and L that have level 2 qualities as shown in Fig. 8. Configurations B and U, however, do not satisfy the specified bounds of Eq. (7), whereas configurations N and U do. The acceleration ratio thus can be used as a test for normal/abnormal response as described by pilot comments.

In summary, the metrics used in the context of roll performance using Gibson's method are given in Table 2.

V. Frequency-Response Analysis

Gibson's frequency analysis does not deviate much from that of pitch axis, except that it includes the roll-acceleration frequency resonse to identify ratcheting phenomena that are unique to the roll axis. Compensatory tasks, such as precision tracking tasks and approach and landing tasks, consist of an open-loop closure via the pilot in the feedback loop. During the task execution, it is essential that the aircraft have good predictability and a smooth response. Such good behavior is observed to be related to an open-loop frequency response around the crossover region. The crossover point, defined as the point where the frequency ratio has unit gain (0 dB), plays an important role in the analysis of such tasks. Gibson's frequency-domain analysis looks at the open-loop frequency response of roll attitude around the crossover region and relates it to the pilot comments. Deviation from good behavior leads to additional closed-loop control activity and possibly to dynamic instabilities such as PIO and ratcheting.

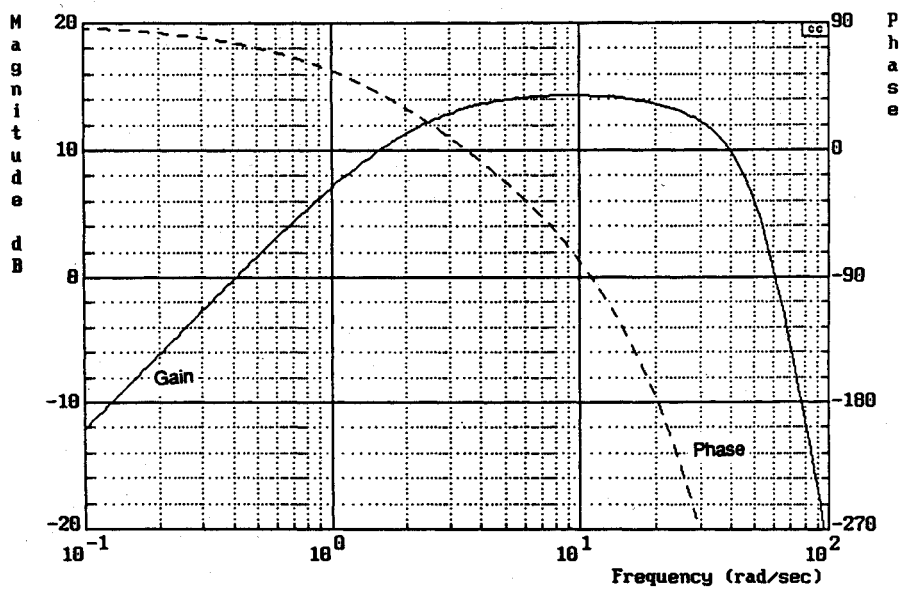

Fig. 9 Roll-acceleration frequency response results (configuration A3).

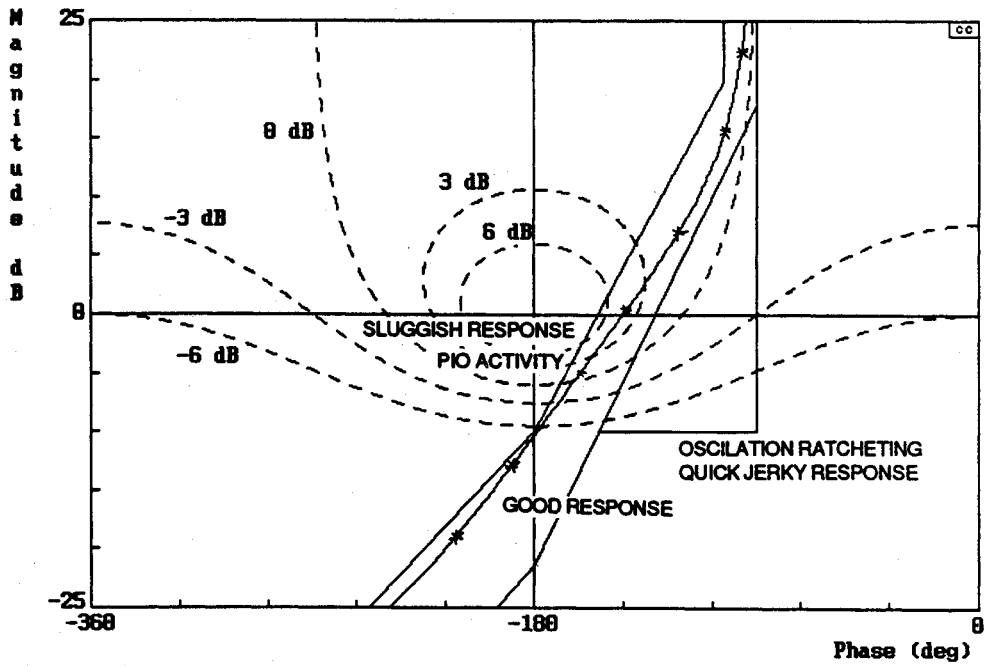

Fig. 10 Roll attitude-frequency response results (configuration J).

The two types of dynamic instabilities exhibited by the roll axis are PIO and ratcheting. PIO is a low-frequency instability and is related to pilot's control activity around the phase crossover region, where the deficiency is caused by the pilot's stick input being out of phase with the aircraft response. The attitude-frequency response shows that this is possible with a rapid increase in phase lag accompanied by a very little gain attenuation around the phase crossover point. Quantitatively, the phase-rate parameter P_r gives excellent correlation with PIO in the pitch axis as well as in roll.[5,6] Phase rate is evaluated using Eq. (2). The other instability, unique to the roll axis, is ratcheting. Historically, roll ratcheting was identified by pilots as a high-frequency PIO. Recent theories indicate that roll ratcheting is excited by the pilot's neuromuscular activity.[11,13] It has been shown that the natural frequency of the neuromuscular system lies in the frequency band from 12 to 18 rad/s.[11] Ratcheting affects the ride qualities but does not endanger the pilot/aircraft system.

Frequency response for roll attitude and roll acceleration are analyzed for all of the tracking configurations. Deficiencies such as PIO and quick and jerky responses are identified by using Nichols charts of roll attitude. The roll attitude-frequency responses are compared for all of the configurations with gain equalization so as to have a gain crossover frequency of 0.3 Hz (0.3 Hz is identified with the pilot's control activity). The same gain adjustment is also used to obtain the roll-acceleration frequency responses, which are necessary to identify ratcheting. Figure 9 shows a typical ratcheting case. From the analysis of roll-acceleration frequency response and stability margins, it is found that the presence of ratcheting occurs if the roll-acceleration crossover frequency lies within the limits

$$12 \text{ rad/s} < \omega_{180} < 18 \text{ rad/s} \tag{9}$$

corresponding to typical pilot's neuromuscular bandwidth. These boundaries can extend to 10 rad/s on the lower side and

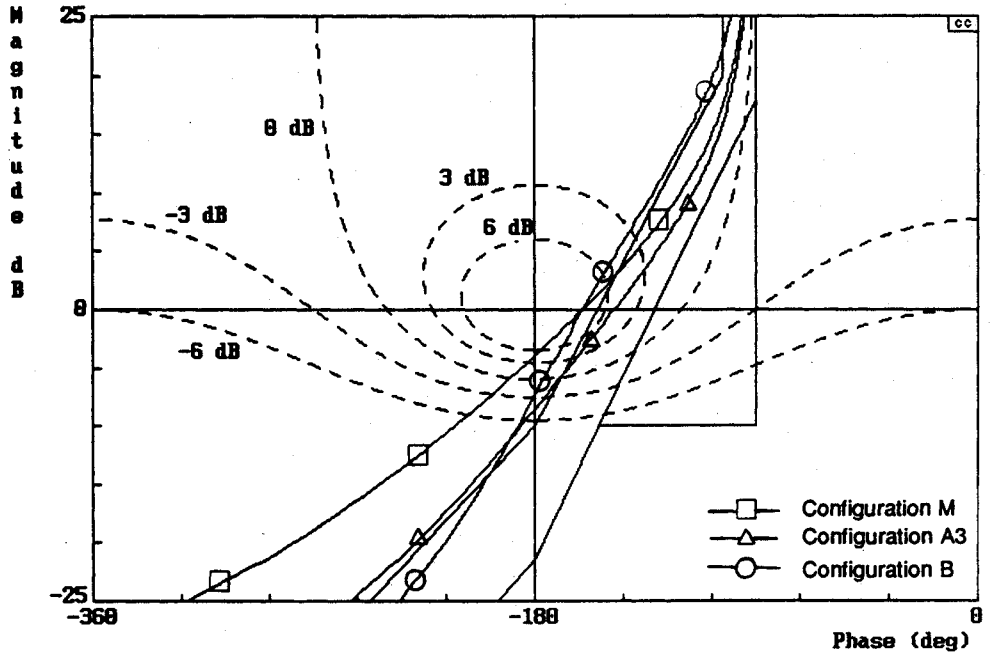

Fig. 11 Roll attitude-frequency response results (configurations M, B, and A3).

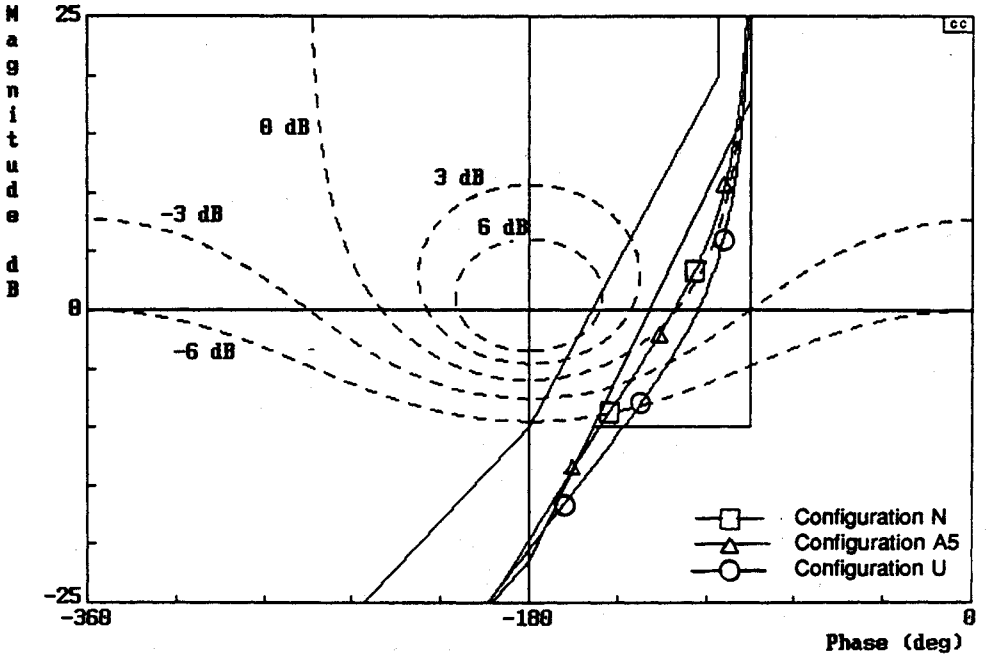

Fig. 12 Roll attitude-frequency response results (configurations A5, U, and N).

Table 3 Limits on roll instabilities

Deficiency	Usage
PIO	$\lvert\ddot{\phi}\rvert \geq -10$ db and $P_r \geq 60$ deg/cps, or $\tau_d \leq 0.03$ s
Ratcheting	$10 \sim 12$ rad/s $\leq \omega_{180} \leq 18 \sim 20$ rad/s

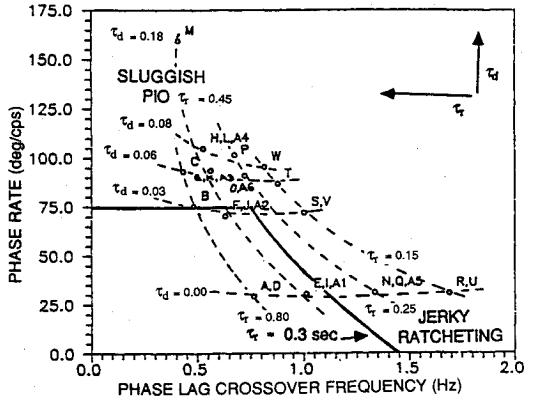

Fig. 13 Phase-rate plot.

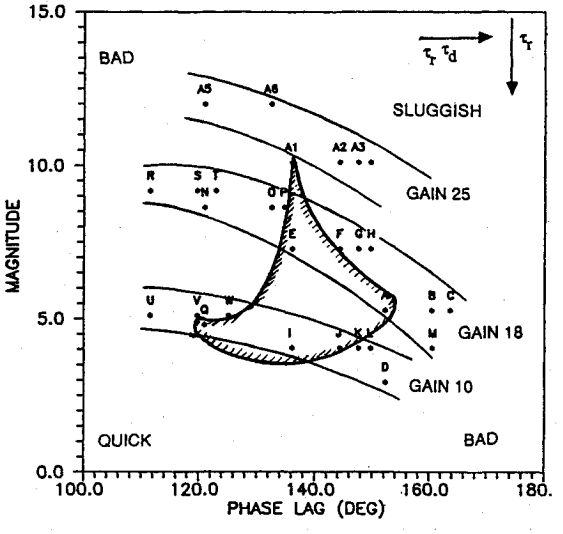

Fig. 14 Thumbprint, function of control sensitivity (level 1 boundaries).

to 20 rad/s on higher side if deficiencies such as PIO, jerky, oscillatory problems exist. The present roll criteria associate ratcheting to a low roll time constant ($\tau_r < 0.3$ s); however, they fail to identify configurations such as Q and A5 ($\tau_r < 0.3$ s) that do not exhibit ratcheting. Ratcheting is also not limited to low τ_r values; for example, configuration A3 ($\omega_{180} = 20$ rad/s) has ratcheting although it has $\tau_r = 0.45$ s. Equation (9) is able to distinguish more accurately the occurrence of ratcheting.

Figure 10 shows the roll attitude-frequency response boundaries. The various regions are labeled showing the nature of the aircraft response. There are three primary regions: 1) sluggish, PIO prone region; 2) optimal tracking region; and 3) quick, oscillatory ratcheting prone region. The central band, which marks a region of good and optimal response, shows a good phase-gain relationship. As an example, Fig. 10 shows configuration J, which exhibits good response. If the attitude plot is to the left or right of the central band, the response of the aircraft becomes less or more sensitive, respectively. To the left of the good response band lies the sluggish, PIO prone zone. Time delay and higher-order terms cause the frequency lines to shift to the left of the central band. Time delay causes a quicker phase-lag increase, with smaller gain attenuation causing sluggish response. The PIO, sluggish response boundary shows good correlation with most of the PIO cases, provided the attitude response is greater than -10 dB. Magnitude less than -10 dB does not affect the pilot comments. Configurations M, B, and A3 (Fig. 11) show various cases of PIO occurrence. Configuration B exhibits pure PIO with comments of sluggish response, whereas configurations M and A3 represent a PIO case accompanied by a possibility of ratcheting. Roll-acceleration plots for M and A3 show that they have a phase crossover frequency of 11 and 20 rad/s, respectively, both lying around the boundary. Thus, ratcheting may or may not be excited. Pilot comments show that A3 has ratcheting, whereas M does not. From the ratcheting condition, it can be concluded that configuration M has a potential for ratcheting deficiency although the pilot comments show the absence of ratcheting. Finally, to the right of the central band is the quick, jerky, oscillatory region that is also shown to encompass configurations with ratcheting. It is worth noting that configurations that are quick, jerky, or oscillatory in nature are invariably remarked as having ratcheting. Configurations A5, U, and N in Fig. 12 clearly show the presence of quick, sharp responses. Configuration A5 confirms with the pilot comments. "Quick, sharp, ratcheting..." comments are observed for configurations U and N. Ratcheting criteria developed above [Eq. (9)] predict the absence of ratcheting for both the configurations U and N. Presently, we are unable to answer this discrepancy, but if we make an assumption that close similarity among the oscillatory and ratcheting response, making it hard for the pilot to distinguish high-frequency ratcheting from the low-frequency sharp oscillatory responses, we are able to get perfect correlation for all of the 29 configurations. This is the reason why Fig. 10 shows the low-frequency quick, jerky response region to be ratcheting also.

The above examples were typical of what can be expected, in general, with frequency-response boundaries showing the general trends in phase lag and magnitude attenuation. Frequency boundary plots, however, do not show the effects of control sensitivity or τ_r or τ_d directly. The effects of variation in roll time constant and time delay on dynamic instabilities is shown in Fig. 13 by plotting phase rate vs phase lag crossover frequency. The phase-rate plot shows τ_r and τ_d isolines; constant τ_r are represented by vertical curves moving to the left as τ_r increases, whereas τ_d are the horizontal curves that shift upward as τ_d increases. From the figure, it is now clear how τ_r affects ratcheting. In fact, the vertical boundary $\tau_r = 0.3$ s is drawn, which approximately represents the new MIL-SPEC lower boundary. The variable τ_d, on the other hand, affects phase rate, which in turn is a function of PIO since phase rate increases with τ_d; large phase rate values cause PIO. The horizontal boundary drawn for $P_r = 75$ deg/cps separates PIO and non-PIO regions.

In the above discussion, roll-control sensitivity was not considered since, in the above analysis, PIO, ratcheting, and oscillations do not depend on it as the pilot in the loop acts as the variable gain controller. To account for sensitivity effects, a thumbprint plot is drawn in Fig. 14. The ordinate of the thumbprint is the gain equalization required to attain a 0.3-Hz crossover, and the abscissa represents the corresponding phase-lag value for the adjusted attitude gain crossover point. The figure shows that configurations are separated in three bands. These bands are the gain sensitivities of the configurations used in the analysis. The central zone identifies the level 1 region and its optimal gain and phase-lag values.

The frequency-response analysis results are summarized in Table 3, which shows ranges of the metrics leading to instability.

VI. Conclusions

An analysis of roll-performance handling qualities was carried out using Gibson's method applied to the LATHOS data base. The method, consisting of a combination of time-do-

main and frequency-domain techniques, has proved to give results consistent with the experimental data. New time-response metrics were introduced to correspond between roll and pitch response and to include control-sensitivity effects. Although only configurations relative to tracking task were considered, the extension to the landing task has shown consistent results that will be reported elsewhere. Gibson's method appears to have a general applicability in both the longitudinal and the lateral planes, and it is an attractive alternative to the modal requirements of present handling-qualities specifications.

Acknowledgments

This work was partially supported by the Auburn University Research Grant-in-Aid, Grant 88-54. The first author wishes to thank J. C. Gibson of the British Aerospace Corporation and John Hodgkinson of McDonnell Douglas for their suggestions.

References

[1]Berry, D. T., "Flying Qualities Criteria and Flight Control Design," *Proceedings of the AIAA Guidance and Control Conference,* AIAA Paper 81-1823, New York, Aug. 1981.

[2]Anon., "Military Specification, Flying Qualities of Piloted Airplanes," MIL-8785C, Nov. 1980.

[3]Hoh, R. H., Mitchell, D. G., Ashkenas, J. L., Klein, R. H., Heffley, R. K., and Hodgkinson, J., "Proposed MIL Standard and Handbook—Flying Qualities of Air Vehicles," Air Force Wright Aeronautical Labs., AFWAL-TR-82-3081, Vol. II, Wright-Patterson AFB, OH, Nov. 1982.

[4]Gibson, J. C., "Flying Qualities and the Fly-by-Wire Aeroplane," AGARD-CP-260, Sept. 1978.

[5]Gibson, J. C., "Piloted Handling-Qualities Design Criteria for High-Order Flight Control Systems," AGARD-CP-333, April 1982.

[6]Gibson, J. C., "Handling Qualities for Unstable Combat Aircraft," *Proceedings of the International Conference of Aeronautical Sciences,* International Council of the Aeronautical Sciences, 86-5.3.4, Sept. 1986.

[7]Mooij, H. A., "Criteria for Low-Speed Longitudinal Handling Qualities of Transport Aircraft with Closed-Loop Flight Control Systems," Ph.D. Dissertation, Delft Inst. of Technology, Delft, The Netherlands, Dec. 1984.

[8]Thukral, A., "Criteria for Lateral Handling Qualities Evaluation," M.S. Thesis, Dept. of Aerospace Engineering, Auburn Univ., Auburn, AL, Sept. 1990.

[9]Booz, J., "Relative Evaluation of MIL-STD-1797 Flying-Qualities Criteria Applicable to Flared Landing and Approach," AIAA Paper 88-4363, Aug. 1988.

[10]Monagan, S. J., et al., "Lateral Flying Qualities of Highly Augmented Fighter Aircraft," Air Force Wright Aeronautical Labs., AFWAL-TR-81-3171, Vol. I, Wright-Patterson AFB, OH, June 1982.

[11]Ashkenas, I. L., "Pilot Modeling Applications," AGARD-LS-157, May–June 1988.

[12]Hodgkinson, J., and La Manna, W. J., "Equivalent System Approaches to Handling-Qualities Analysis and Design Problems of Augmented Aircraft," AIAA Atmospheric Flight Mechanics Conference, Hollywood, FL, Aug. 1977.

[13]Hoh, R. H., "Unifying Concepts for Longitudinal Flying Qualities Criteria," Systems Technology, Inc., Working Paper 503-69, AGARD-FMP, Working Group 17, Oct. 1988.

[14]Innocenti, M., and Thukral, A., "Roll-Response Criteria for High-Maneuverable Aircraft Using Gibson's Method," AIAA Paper 89-3391, Aug. 1989.

[15]Smith, R. E., "Effects of Control Systems Dynamics on Fighter Approach and Landing Longitudinal Flying Qualities," Air Force Flight Dynamics Lab., AFFDL-TR-78-122, March 1978.

[16]Rynaski, E. G., "Flying Qualities and Flight Control," Calspan Final Rept. 7205-8, Contract F33615-83-C-3603, March 1985.